Massachusetts Institute of Technology.
Dept. of Earth and Planetory Sciences.
Estimation of earthquake risk.

Department of Earth and Planetary Sciences

Massachusetts Institute of Technology

Cambridge, Massachusetts 02139

FINAL REPORT

to

National Oceanic and Atmospheric Administration

NOAA Contract No. N22-163-72-G

ESTIMATION OF EARTHQUAKE RISK

1 June 1972 - 30 June 1974

6 January 1975

ABSTRACT

Statistical modeling of earthquake occurrences is studied. First a statistical method of detecting dependent events and aftershocks using spatial and temporal information was developed and applied to Japan and California earthquake catalogs. On the basis of a statistic s

$$s = \pi r^2 kt$$

where r is the distance between two events, k is the normal earthquake rate and t is the time interval between the events, a decision was made whether a pair of events were dependent. The theoretical distribution of s for a catalog consisting of only independent events was compared to the actual catalogs. On the basis of the differences between the distributions, the number of inferred dependent events was determined.

This discrimination technique was applied to the earthquake catalogs of Northern Japan (1926-1960) and Southern California (1934-1960). Thirty percent of all events in the Japan catalog and 42 percent of events in the Southern California logs were identified as dependent events.

The statistical properties of the catalogs without dependent events were examined, in particular with respect to the Poisson process. Some small discrepancies with the Poisson process still existed using a decision threshold of s = 0.02. Clusters of events were found that could not be related to any large magnitude main event.

For modeling of earthquake and aftershock occurrences a compound Poisson-Markov process was examined. The state variable for the Markov model was assumed to be the accumulated strain energy ε. Suitable functions $\lambda(\varepsilon)$ and $T(X|\varepsilon)$, the rate and transition probabilities respectively, were chosen to duplicate the known decay relation for aftershock sequences and the frequency magnitude relation. It was found that in order for large ε to accumulate it was necessary for energy to be put into the model in sudden bursts.

The model was simulated on a computer using a random number generator. Catalogs generated in this way departed from the real catalog in only one manner, namely that large aftershocks inhibit rather than trigger subsequent aftershocks.

TABLE OF CONTENTS

I. INTRODUCTION

The main thrust of this project has been to produce statistical models for earthquake occurrences. Such theoretical models enable one to reduce large data sets to theoretical parameters that describe the earthquake occurrences. These can be used for prediction of earthquake occurrences and risk analysis. Furthermore, they can be related to physical phenomena that control the occurrences.

The theoretical modeling of earthquake occurrences first of all requires identification of "independent events" or "prime earthquakes" as opposed to aftershocks strongly dependent on these "independent events." Although the total number of earthquakes is of interest in generating synthetic catalogs, the "prime earthquakes" are most important in risk analysis. Under this project our studies were primarily channeled to two specific topics:

1. Developing a statistical method for identifying dependent events and aftershocks, and
2. Generating a compound Poisson-Markov model of earthquake occurrences. These are described in detail in the next two sections.

II. A STATISTICAL METHOD OF IDENTIFYING DEPENDENT EVENTS AND EARTHQUAKE AFTERSHOCKS

Introduction

The occurrences of shallow earthquakes are not random in time and space. The existence of aftershock sequences and earthquake swarms have been known for a long time. Statistical studies of earthquake occurrences have shown that they are in gross disagreement with the Poisson process (Shlien and Toksöz, 1970; Utsu, 1972; and Vere-Jones and Davies, 1966). The main cause of this disagreement is attributed to clustering of these events due to the presence of aftershocks and earthquake swarms.

There are at least two reasons why it is important to be able to detect and remove the earthquake clusters from the catalogs. First the clustering has a large first order effect on the statistics of earthquake occurrences that may conceal less dominant patterns in the earthquake catalog such as periodicities and gaps in earthquake activity. Second, in estimating the seismic risk in a region one may wish not to include related events such as aftershocks and swarms, since these events have lesser effect than the main shocks and their inclusions affect the recurrence times.

Attempts have been made by Knopoff and Gardner (1972), Keilis-Borok et al. (1972), and Utsu (1969) to remove these aftershocks. These have relied on the same basic approach for eliminating the dependent events. The earthquake catalog was searched for large magnitude events and then all other events that were listed within some prescribed distance and time of the large earthquake were removed from the catalog. This scheme was not effective in eliminating earthquake swarms which are not necessarily related to any specific high magnitude event. Shimazaki (1973) applied a more statistical scheme but based on temporal information only.

In this paper we investigate an alternative approach which includes both space and time information (but not the magnitude constraints) for identifying dependent events.

We first describe the basic method to identify related events and determine the theoretical properties of this discriminant. We then apply this scheme to the Japan Meteorological Agency (JMA) shallow earthquake catalog of Northern Japan (1926-1960) and to a catalog of earthquakes in Southern California (1934-1963).

Detection of Dependent Events

The discrimination scheme that was studied can be most easily understood geometrically. Let earthquakes be represented by points in a three dimensional space in which the vertical axis is time and the horizontal coordinates are related to the spatial position of the epicenter. If the events occur independently in time and space then one can make quantitative predictions of the spacing of these points on the basis of the seismicity distribution. In particular the probability of one or more points falling in a given volume V is given by

$$P(V) = \exp(-\int_V k(x,t)\, dx\, dt) \qquad (1)$$

where k(x,t) is the rate of earthquake occurrences at time t and position x (Keilis-Borok et al. 1972). Assuming a stationary model in time then

$$k(x,t) = k(x) \qquad (2)$$

The volume V in consideration is completely arbitrary. If one is given the fact that an earthquake occurred in a specific volume, then the probability of any other independent event appearing in the same region P(V|E) should be P(V). On the other hand, if there is a definite clustering of events in time and space then the observed probability P(V) would definitely be larger if the volume contains the given event. To determine whether events are occurring independently or not it is necessary to compare P(V) with its theoretical distribution. Using this approach Keilis-Borok et al. (1972) proved the interrelatedness of earthquake occurrences.

The volume should be shaped such that it would most likely include an event related to a given earthquake if one exists. In this study, the particular volume that was selected was one that would detect both distant related events occurring within a short time of the given event and nearby events that occurred considerably later. The region was defined by the equations

$$S = \pi r^2 tk \leq \alpha$$

$$r \leq R_{max} \qquad (4)$$

$$0 \leq t \leq T_{max}$$

where r and t are the distance and time intervals between the two events, k is the average seismicity associated with the area and α, R_{max}, and T_{max} were the thresholds chosen in advance. The region is illustrated schematically in Figure 1.

To determine whether a specific event could be related to an earlier event a search was made for all past events satisfying all the relations given in (4). If such an earlier event could be found, then the specific event was assumed to be dependent. In cases of earthquake swarms or aftershock sequences, it was not uncommon to be able to relate the specific event to several previous events. Using a suitable bookkeeping procedure all the events associated with a specific cluster were recorded.

The procedure would of course relate independent events occasionally. By applying equation (1) and letting

$$T_{max} = \frac{\alpha}{\pi k R_{max}^2} \quad A \qquad (5)$$

where A is a chosen constant, then the probability of a spurious cluster detected at any specific point is

$$P(\alpha,A) = 1 - \exp(-\alpha(\ln A + 1)) \qquad (6)$$

This result is derived in the appendix. In this investigation α, A, R_{max} were given the values: $\alpha = 0.02$, $A = 100$, and $R_{max} = 1.41$ degrees. These yield $P(\alpha,A) = 0.10$.

Application to Japan and Southern California Earthquakes

The above scheme was applied to two local earthquake catalogs for which data was available over an extensive period of time. The two areas were (1) the area covering the Southern end of Hokkaido and the Northern section of Honshu, Japan, for the period 1926-1960 and (2) Southern California 1934-1963. These areas are shown in Figures 2a and 2b. The data were obtained from the Japan Meteorological Agency (JMA) shallow earthquake catalog and the catalog of earthquakes in Southern California.

The seismic rate k in equation (4) was estimated from the total number of events in rectangular sectors 1° latitude by 1° longitude for Northern Japan and 0.5° by 0.5° for Southern California. (Small changes in the area of the sectors due to the sphericity of the earth were neglected.) At any given point the seismic rate k was determined using a bilinear interpolation. The k parameter used in equation (4) was that associated with the epicenter of the earlier event. This approximation is valid provided that k does not vary rapidly in the area of interest. By requiring that r in equation (4) is less than $\sqrt{2}$ degrees, the error in this approximation was kept small.

The initial k estimate was based on both dependent and independent events. In cases where aftershocks dominate the catalog it may be desirable to apply the discrimination scheme twice on the entire catalog. On the second pass, the k estimates would be based on only the events that were classified as independent in the first pass.

The scheme was tested initially on a synthetic earthquake catalog which had the same spatial seismic distributions as in the original Japan and California catalogs. The synthetic catalogs were generated by a Monte Carlo scheme using a random number generator. All the events in the synthetic catalog were generated independently of each other by a Poisson model so that there were no aftershocks or swarms. Accordingly, the probability distribution function of the decision parameter s should be the same as α given in equation (6). In Figure 3, the probability functions of s determined from the synthetic and original catalogs are indicated by 'o' and 'x' respectively. The smooth curve is the theoretical distribution for the independent events. The s distribution determined from the synthetic catalogs are in close agreement with the theoretical model.

The s distribution of the actual catalogs definitely departs from the model of completely independent events. About 30 percent of the events in the JMA catalog and 42 percent of the events in the catalog of earthquakes in Southern California had an s value below $\alpha = 0.02$. To eliminate the dependent events, all events that had an s value below $\alpha = 0.02$ were categorically classified as dependent events and removed from the catalog. This scheme would eliminate 10 percent of the events in a catalog consisting entirely of statistically independent events.

The Southern California catalog of earthquakes was different from the JMA catalog in the sense of covering a smaller area and reporting events down to magnitude 3. Since the JMA catalog did not report many events below magnitude 5 in the 1926-1960 time period, it was less dominated by earthquake swarms and aftershocks.

The statistical properties of the filtered catalog were compared with those of the original catalog and with those of a Poisson process. The autocorrelation function C(k) was evaluated using equation (7)

$$C(k) = \frac{\sum_{i=1}^{N-k} (n(i) - \langle n(i) \rangle)(n(i+k) - \langle n(i+k) \rangle)}{(N-k)\ \mathrm{var}\ (n(i))} \qquad (7)$$

where n(i) is the number of events in the i th non-overlapping time unit (here 0.2 months), $\langle . \rangle$ denotes the arithmetic mean and var (.) denotes the variance of the term in parentheses. If the Poisson assumptions are satisfied then C(k) for k different from zero should be normally distributed about zero with variance $\frac{1}{N-k}$ (Box and Jenkins, 1970). The Poisson index of dispersion defined as the ratio of the variance to mean of n(i) should be unity.

In Figures 4 and 5 the autocorrelation functions were plotted for the original and filtered catalogs in Japan and California. The removal of the dependent events reduced the high autocorrelation peaks. The autocorrelation function of the filtered JMA catalog appears to be generally within the 95 percent statistical limits indicated, however the autocorrelation function of the Southern California catalog has a positive trend which is still apparent in the second pass. The large peak at 20 months lag (Figure 5) in the original catalog corresponded to the time interval between the Kern County earthquake (21 July 1952) and the Santa Rosa earthquake (19 March 1954) which had many aftershocks.

The greater difficulty in whitening the statistical properties of the Southern California catalog can be explained by the much more extensive aftershock sequences. For example, the Kern County aftershock sequence beginning July 1952 extended over 40 months in the catalog. In Figure 6, the number of earthquakes per month in the vicinity of the Manix fault, (34.0-35.0N, 116.5-117.0W) California was plotted for the original and filtered catalogs. The aftershock sequences to the earthquake 10 July 1947 are very prominent in the original catalog, are still noticeable in the first pass, and are barely discernable in the second pass.

The Poisson index of dispersion was calculated as a function of the time interval using equations (8) and (9).

$$D(kt) = \frac{var\ (n(kt))}{\langle n(kt)\rangle} \tag{8}$$

$$var(n(kt)) = k\ var\ (n(t)) + 2 \sum_{j=1}^{k-1} (k-j)\ C(j) \tag{9}$$

where n(t) is the number of events in a time interval t. The Poisson index of dispersion is very sensitive to regular departures of the autocorrelation function from the expected zero value. In Figures 7a and 7b the Poisson index of dispersion is plotted versus time for the JMA and Southern California catalogs. For a Poisson process D(t) has a certain distribution about 1. If there are M non-overlapping intervals of length t, MD(t) is χ^2 distributed with M-1 degrees of freedom. The filtered JMA catalog was found acceptable with the Poisson model at a 95% significance for t less than 4 months but the filtered California catalog (2nd pass) was still unacceptable at the 95% level for all t greater than a month.

In order to be able to evaluate quantitatively the efficiency of any particular discriminant of independent from related events it is necessary to know in advance in which category any particular event belongs. Unfortunately this information is unknown due to the lack of any precise definition of an aftershock. The statistical properties of aftershock sequences and earthquake swarms are so variable that no exact definition seems possible.

The catalog of earthquakes in Southern California can be made more Poisson-like at the expense of losing more independent events, by raising the threshold α. Whether this is desirable depends on the actual application that one has in mind. If too large an α is used then $D(t)$ may become less than 1, indicating a lack of events occurring within short times of each other.

In this study, it was found that large clusters of earthquakes are not necessarily associated with large events and vice-versa. For example, in Southern California a cluster of 38 events with magnitudes between 2 and 3 were found to occur at 35.7N 118.3W beginning 10 May 1935. The largest event in that area, magnitude 4.0 occurred one month later and was followed by only two aftershocks. Conventional methods of detecting aftershocks that use the magnitude of the main shock would fail to detect that cluster. Instances of magnitude 5.0 earthquakes occurring with two or less aftershocks were not found to be exceptional in the California catalog. Similar cases were found in the JMA catalog. None of the events were reported to be deep.

Conclusions

A statistical method of detecting dependent events and aftershocks using spatial and temporal information was applied to portions of the Japan Meteorological Agency shallow earthquake catalog 1926-1960 and the catalog of earthquakes in Southern California 1934-1963. Applying a decision rule

$$S = \pi r^2 kt < 0.02$$

$$r < \sqrt{2} \text{ degrees}$$

$$t < \frac{1}{\pi k}$$

30 percent of the events in the JMA catalog studied were found to be dependent and 42 percent of the events in the catalog of earthquakes in Southern California. On similar catalogs consisting of independent events only 10 percent of the events would satisfy the above dependent criteria.

Elimination of the dependent events gave the JMA catalog a more Poisson appearance. However, the filtered Southern California catalog still had a non-Poisson component.

It was observed that large clusters of events were not always associated with large earthquakes and vice-versa.

The presence of large aftershock sequences in earthquake catalogs introduces transient effects that one may wish to eliminate. For example the twenty month peak in the auto-correlation function for the Southern California area (Figure 5) was the result of two aftershock sequences spaced twenty months apart. In searching for seismicity gaps in space and time, the presence of clusters of dependent events will bias the results. For such studies the elimination of the dependent events from earthquake catalogs would be valuable.

Acknowledgements

We would like to thank Mr. K. Shimazaki of Tokyo Earthquake Research Institute and Prof. A. Cornell of the Civil Engineering Department, M.I.T. for providing us with copies of the Japan Meteorological Agency shallow earthquake catalog, and catalog of earthquakes in Southern California.

This work was supported by the National Oceanic and Atmospheric Administration under contract N22-163-72-G.

References

Box, G.E.P. and G.M. Jenkins (1970). Time Series Analysis Forecasting and Control. Holden-Day.

Keillis-Borok, V.I., V.M. Podgaetskaya, and A.G. Prozorov (1972). Local statistics of earthquake catalogs. In Computational Seismology, Keilis-Borok (ed.), p. 214. Plenum Publishing, New York.

Knopoff, L. and J.K. Gardner (1972). Higher seismic activity during local night on the raw worldwide earthquake catalog. Geophys. J.R. Astro. Soc. 28, 311-313.

Shimazaki, K. (1973). Statistical method of detecting unusual seismic activities. Bull. Seism. Soc. Am. 63, 969-982.

Shlien, S. and M.N. Toksöz (1970). A clustering model of earthquake occurrences. Bull. Seism. Soc. Am. 60, 1765-1787.

Solov'ev, S.L. and O.N. Solov'eva (1962). Exponential distribution of the total number of earthquake's aftershocks and the decrease of their mean value with increasing depth. Bull. Academy of Sciences USSR Geophysics Series 7, 1053-1059.

Utsu, T. (1972). Aftershock and earthquake statistics IV J. Faculty of Science, Hokkaido University, Geophysics Series 7 Vol. 4 No. 1, 1-42.

Vere-Jones, D. and R.B. Davies (1966). A statistical survey of earthquakes in the main seismic region of New Zealand. Part 2. Time Series Analysis New Zealand J. Geol. Geophys. 9, 251-284.

Appendix

The probability of the decision parameter s exceeding the threshold can be determined analytically assuming complete independence of events in time and space. The conditions given by equation (10)

$$S = \pi r^2 Rt < \alpha$$
$$r < R_{max}$$
$$t < T_{max} = \frac{\alpha A}{\pi k R^2_{max}} \qquad (10)$$

define the region shown in Figure 1. Assuming that k is the average density of events in this region of volume V then the probability of one or more events occurring in this region is given by equation (11)

$$P(V) = 1 - \exp(-kV) \qquad (11)$$

(Keilis-Borok, 1972). It remains to determine the volume V of this region.

$$V = \int_{\tau}^{T_{max}} \pi r^2(t)dt + \pi\tau R^2_{max}$$
$$= \int_{\tau}^{T_{max}} \frac{\alpha}{tk}\, dt + \pi\tau R^2_{max}$$
$$= \frac{\alpha}{k} \ln(T_{max}/\tau) + \pi\tau R^2_{max} \qquad (12)$$

where $\tau = \dfrac{\alpha}{\pi k R^2_{max}}$. If we allow T_{max} to be a function of k such that

$$\frac{T_{max}}{\tau} = A.$$

then the volume is given by

$$V = \frac{\alpha}{k}\,(\ell nA + 1)$$

and the probability of finding one or more events in the volume is

$$P(\alpha) = 1 - \exp(-\alpha(\ell nA + 1))$$

Figure Captions

Fig. 1 Decision region to accept the hypothesis that a pair of events belong to the same cluster. t is the time interval and r is the distance between the events.

Fig. 2a Number of earthquakes per year (upper number) and mean magnitude (lower number) of earthquakes in 1° by 1° rectangular sectors in Northern Japan.

Fig. 2b Number of earthquakes per year and mean magnitude of earthquakes in 0.5° by 0.5° rectangular sectors in Southern California.

Fig. 3 The incremental probability distribution of the decision statistic s for Northern Japan (left) and Southern California (right). The 'x' -s were determined from the actual catalogs, the 'o' -s were determined from a synthetic catalog and the smooth curve is the theoretical distribution assuming independent events.

Fig. 4 Autocorrelation function of the number of earthquakes per 0.2 months determined from the original JMA catalog (top) and from the filtered JMA catalog (bottom).

Fig. 5 Autocorrelation function of the number of earthquakes per 0.2 months determined from the original catalog of earthquakes in Southern California (top) and from the filtered catalog of earthquakes in Southern California (bottom).

Fig. 6 The number of earthquakes per month in a sector 0.5° by 0.5° in the area centered at the Manix fault (34.0 - 34.0 N 116.5 - 117.0 W). The top graph was determined from the original catalog; the middle graph was determined from the filtered catalog for which the seismic rate k included all events, and the bottom graph was determined from the filtered catalog for which the seismic rate k only included independent events.

Fig. 7a Poisson index of dispersion as a function of time interval determined from the original and filtered JMA catalogs 1926-1960.

Fig. 7b Poisson index of dispersion as a function of time interval, determined from the original and filtered catalogs of earthquakes in Southern California 1934-1963.

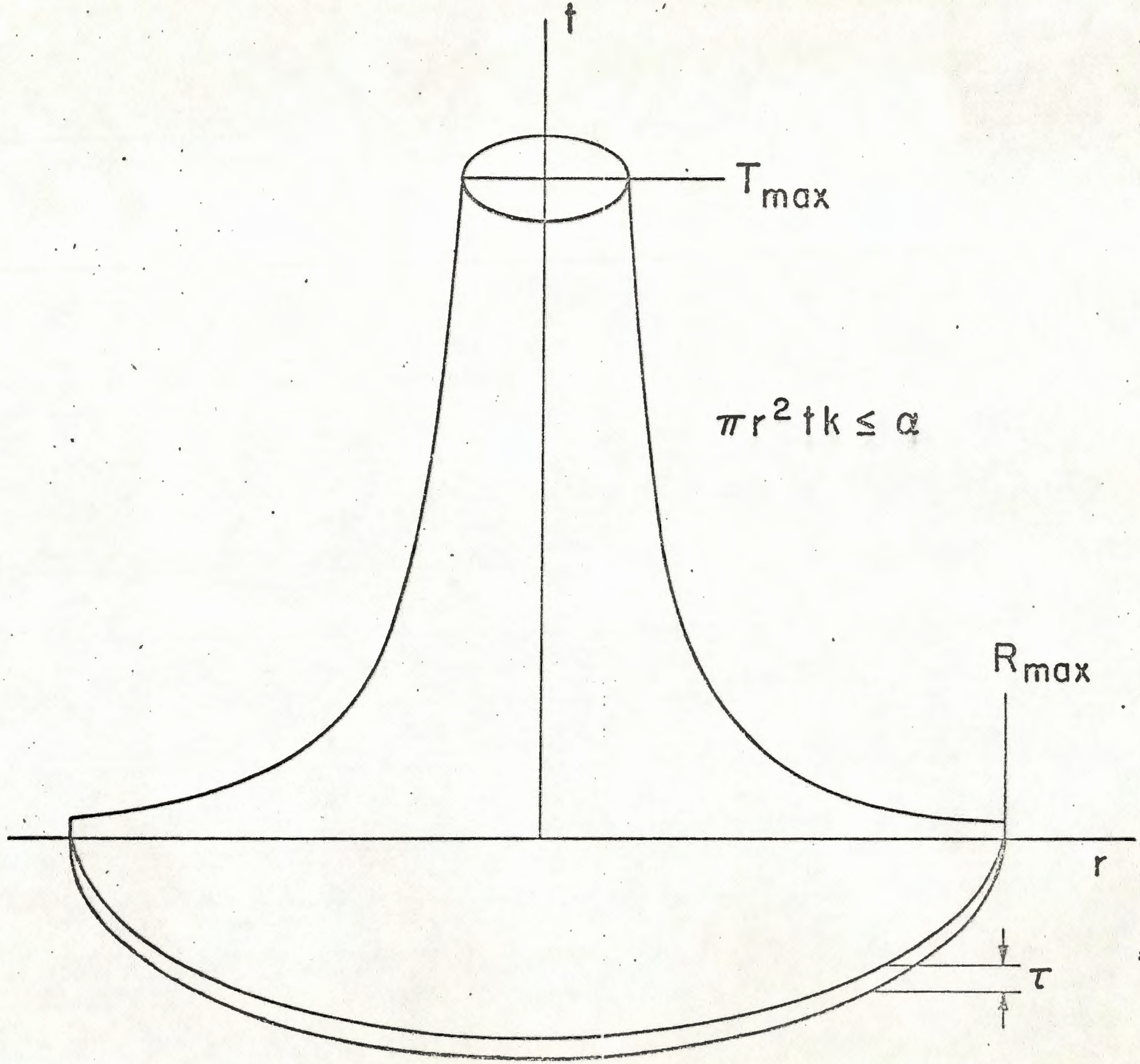

Fig. 1

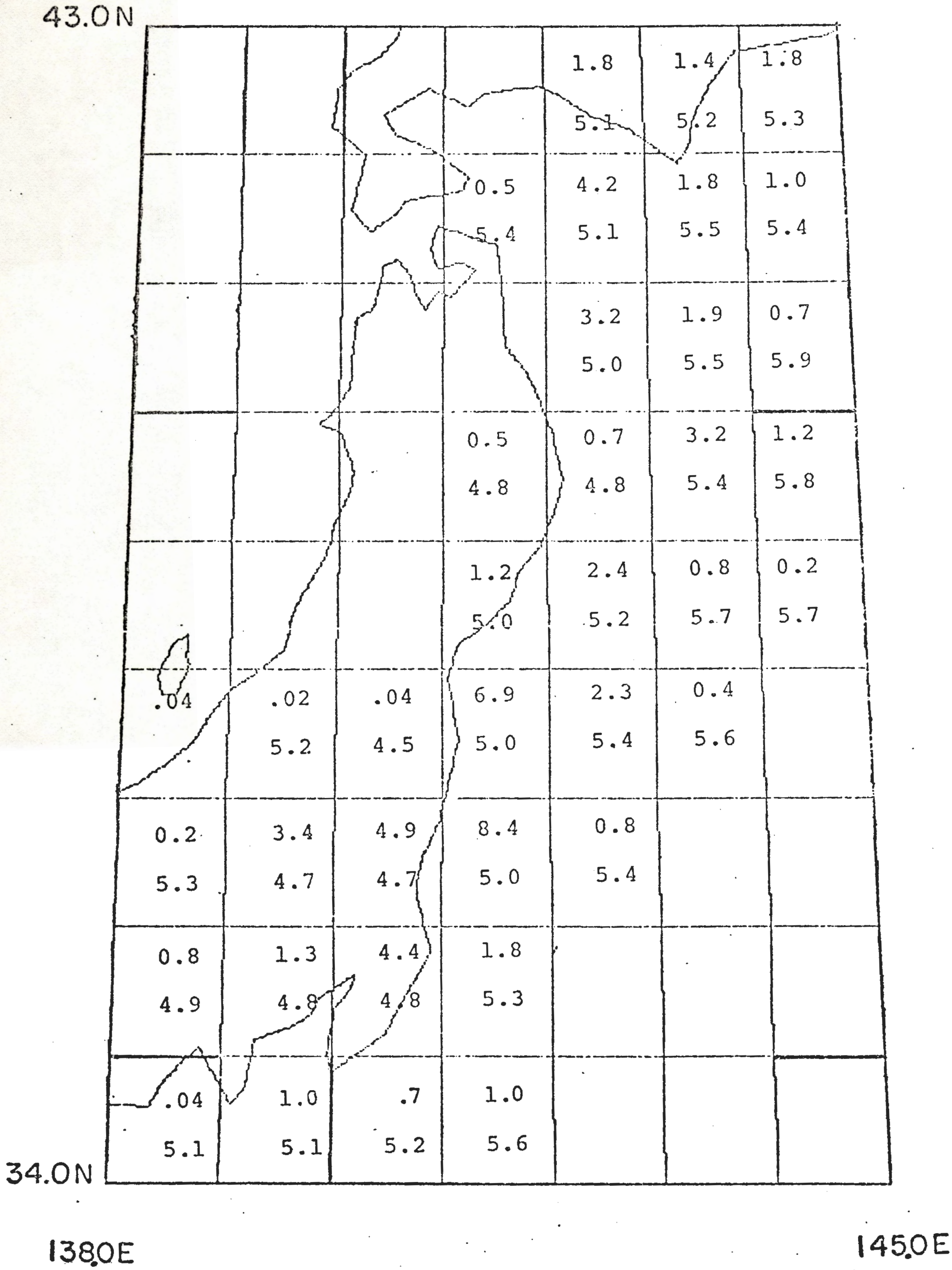
43.0N
1.8 1.4 1.8
5.1 5.2 5.3
0.5 4.2 1.8 1.0
5.4 5.1 5.5 5.4
3.2 1.9 0.7
5.0 5.5 5.9
0.5 0.7 3.2 1.2
4.8 4.8 5.4 5.8
1.2 2.4 0.8 0.2
5.0 5.2 5.7 5.7
.04 .02 .04 6.9 2.3 0.4
5.2 4.5 5.0 5.4 5.6
0.2 3.4 4.9 8.4 0.8
5.3 4.7 4.7 5.0 5.4
0.8 1.3 4.4 1.8
4.9 4.8 4.8 5.3
.04 1.0 .7 1.0
5.1 5.1 5.2 5.6
34.0N
138.0E
145.0E

Fig. 2a

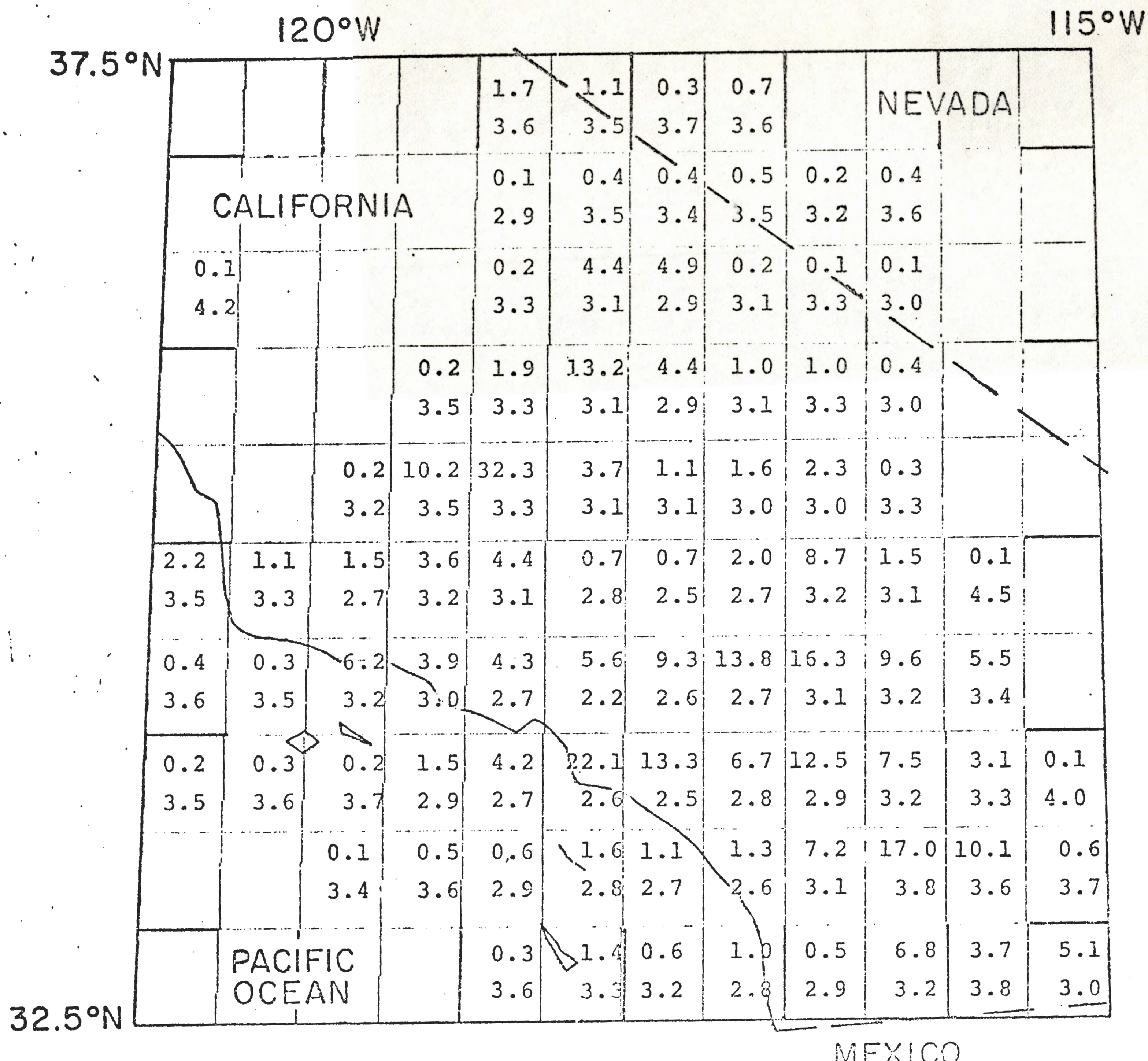

120°W
115°W
37.5°N
32.5°N
CALIFORNIA
NEVADA
PACIFIC OCEAN
MEXICO
1.7 1.1 0.3 0.7
3.6 3.5 3.7 3.6
0.1 0.4 0.4 0.5 0.2 0.4
2.9 3.5 3.4 3.5 3.2 3.6
0.1 0.2 4.4 4.9 0.2 0.1 0.1
4.2 3.3 3.1 2.9 3.1 3.3 3.0
0.2 1.9 13.2 4.4 1.0 1.0 0.4
3.5 3.3 3.1 2.9 3.1 3.3 3.0
0.2 10.2 32.3 3.7 1.1 1.6 2.3 0.3
3.2 3.5 3.3 3.1 3.1 3.0 3.0 3.3
2.2 1.1 1.5 3.6 4.4 0.7 0.7 2.0 8.7 1.5 0.1
3.5 3.3 2.7 3.2 3.1 2.8 2.5 2.7 3.2 3.1 4.5
0.4 0.3 6.2 3.9 4.3 5.6 9.3 13.8 16.3 9.6 5.5
3.6 3.5 3.2 3.0 2.7 2.2 2.6 2.7 3.1 3.2 3.4
0.2 0.3 0.2 1.5 4.2 22.1 13.3 6.7 12.5 7.5 3.1 0.1
3.5 3.6 3.7 2.9 2.7 2.6 2.5 2.8 2.9 3.2 3.3 4.0
0.1 0.5 0.6 1.6 1.1 1.3 7.2 17.0 10.1 0.6
3.4 3.6 2.9 2.8 2.7 2.6 3.1 3.8 3.6 3.7
0.3 1.4 0.6 1.0 0.5 6.8 3.7 5.1
3.6 3.3 3.2 2.8 2.9 3.2 3.8 3.0

Fig. 2b

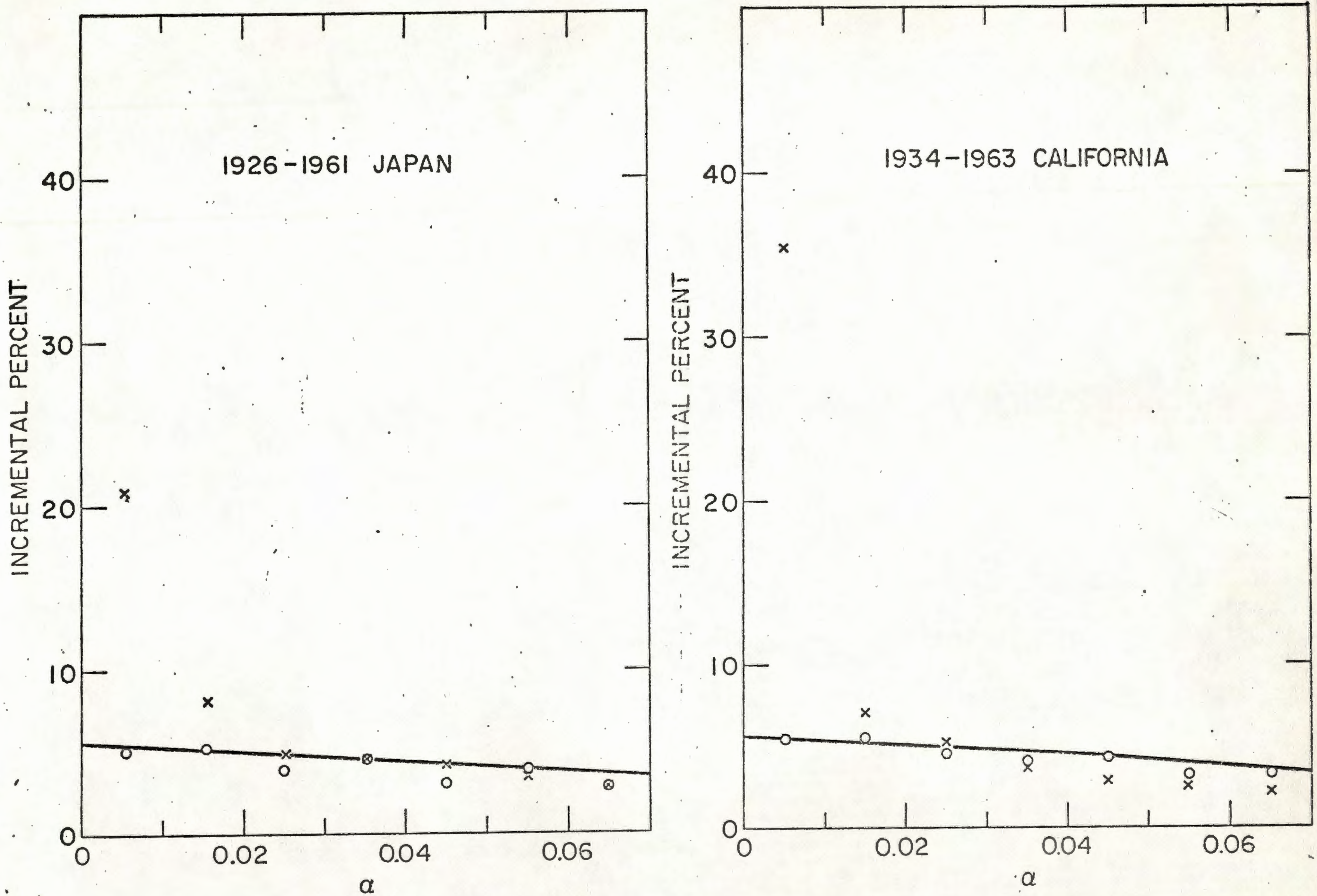
1926-1961 JAPAN
1934-1963 CALIFORNIA
INCREMENTAL PERCENT
0
10
20
30
40
0
0.02
0.04
0.06
α

Fig. 3

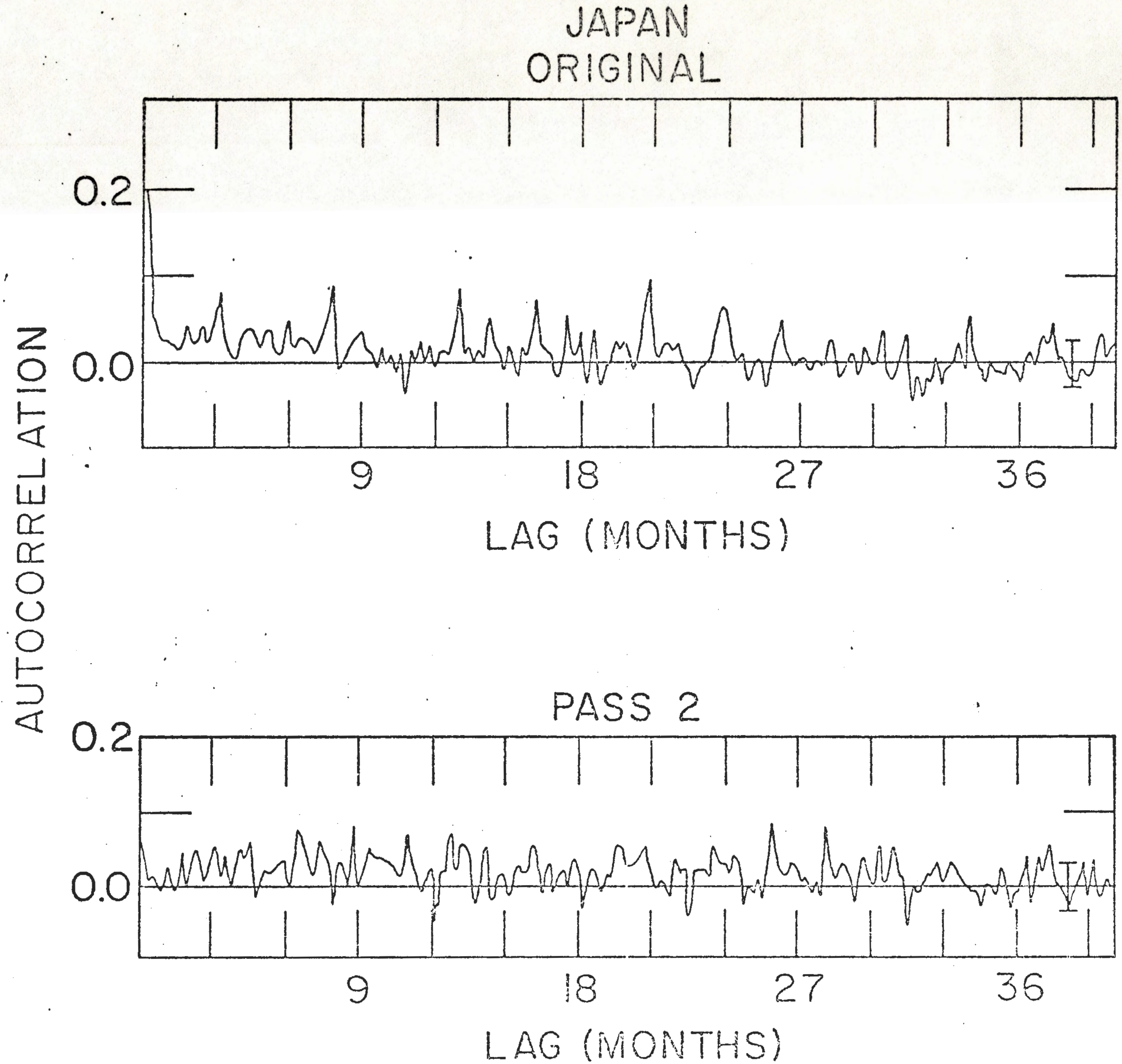
JAPAN
ORIGINAL
0.2
0.0
9
18
27
36
LAG (MONTHS)
AUTOCORRELATION
PASS 2
0.2
0.0
9
18
27
36
LAG (MONTHS)

Fig. 4

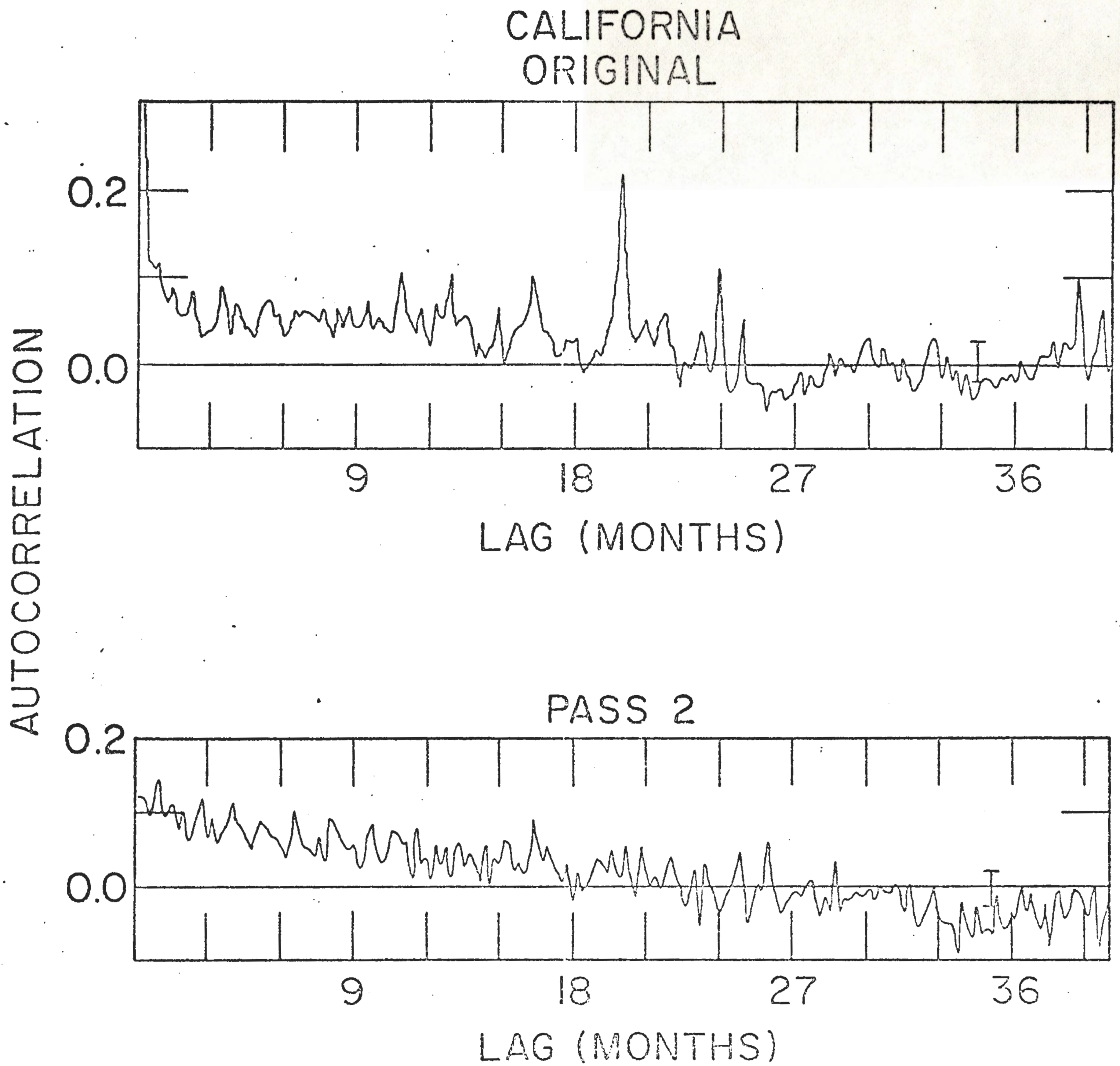
CALIFORNIA
ORIGINAL
0.2
0.0
9
18
27
36
LAG (MONTHS)
AUTOCORRELATION
PASS 2
0.2
0.0
9
18
27
36
LAG (MONTHS)

Fig. 5

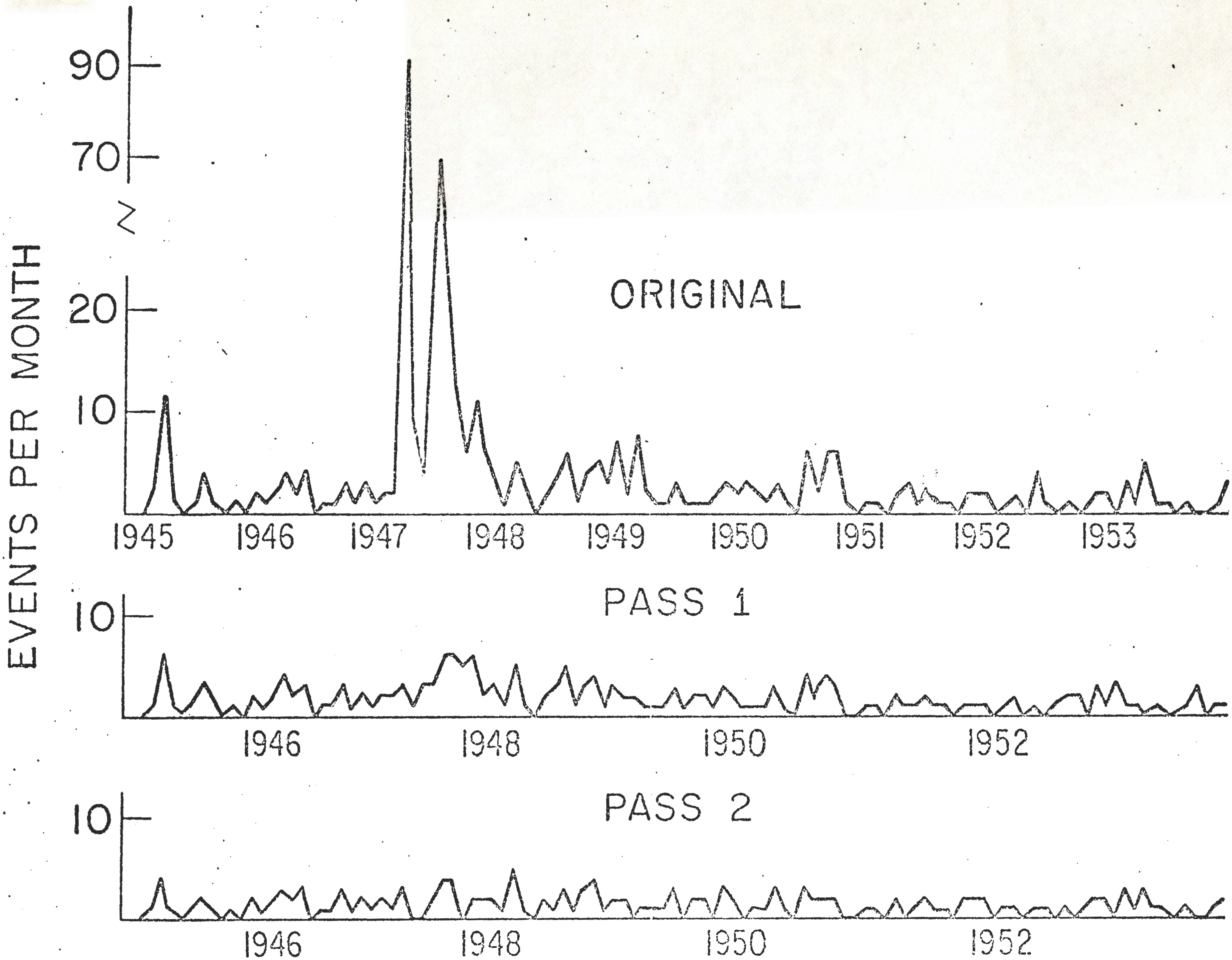
EVENTS PER MONTH
90
70
20
10
ORIGINAL
1945
1946
1947
1948
1949
1950
1951
1952
1953
PASS 1
10
1946
1948
1950
1952
PASS 2
10
1946
1948
1950
1952

Fig. 6

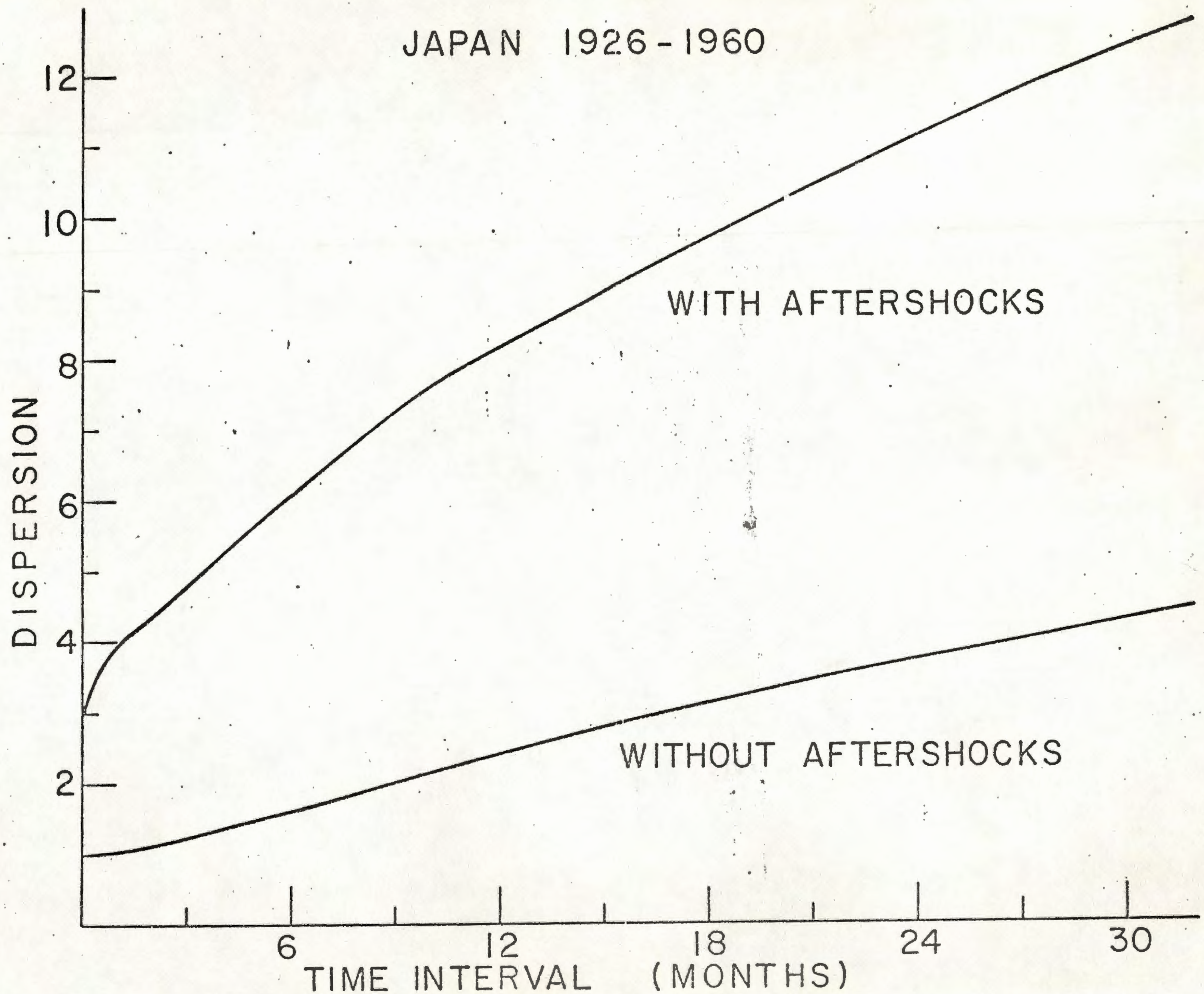
JAPAN 1926-1960
DISPERSION
12
10
8
6
4
2
WITH AFTERSHOCKS
WITHOUT AFTERSHOCKS
6
12
18
24
30
TIME INTERVAL (MONTHS)

Fig. 7

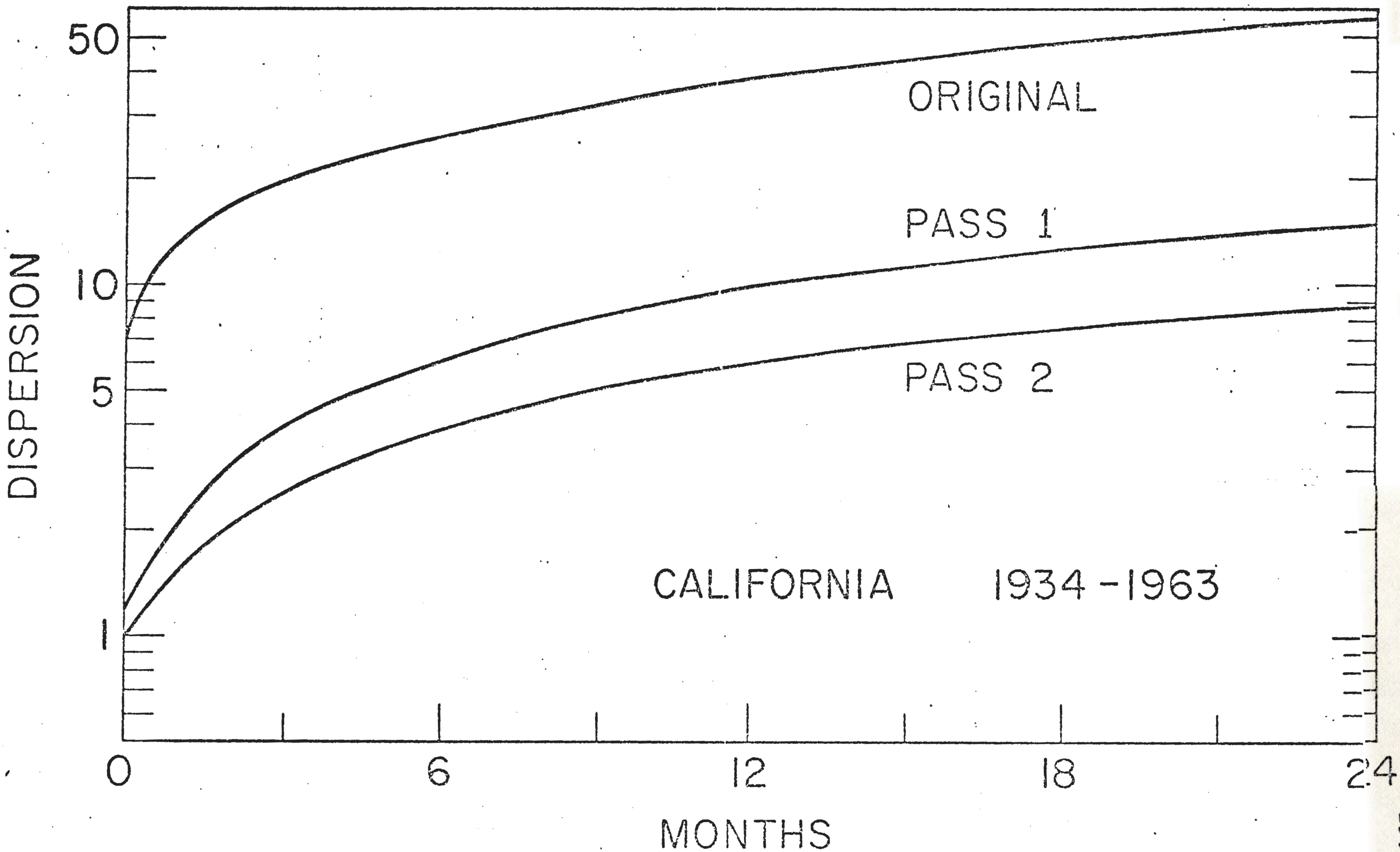
50
10
5
1
DISPERSION
ORIGINAL
PASS 1
PASS 2
CALIFORNIA 1934-1963
0
6
12
18
24
MONTHS

Fig. 7b

III. A BRANCHING POISSON-MARKOV MODEL OF EARTHQUAKE OCCURRENCES

INTRODUCTION

With the ever growing amount of earthquake data becoming available, statistical models of earthquake occurrences have been gaining greater importance. Statistical models allow one to reduce large data sets of earthquake occurrences to statistical parameters that describe these occurrences in a given region. They can be used to predict earthquake occurrences, maximum ground motions and earthquake hazard at a given region (Cornell 1968; Algermissen 1969; Milne & Davenport 1969).

Recently there has been considerable interest in developing a Markov model of earthquake occurrences (Aki 1956; Filson 1973; Knopoff 1971; Knopoff *et al*. 1972; and Vere-Jones, 1966, 1970). Unlike models based on the Poisson model (Shlien & Toksöz 1970), the Markov model, as will be shown, can be used to explain both the frequency magnitude distribution and the occurrence of aftershocks. More flexibility is offered by the Markov process allowing one to put a greater physical basis on the mathematical model.

According to Mogi's hypothesis (1967) when a large event occurs, a major portion of the accumulated strain energy is released. The remaining part of this energy is released more gradually by a series of aftershocks in the source region. The release of this energy by aftershocks follows some definite empirical relations and can be modelled by a Markov process.

The basis of the Markov process is a state variable ε which describes the state of the process at any given instant of time, and a transition function $T(X|\varepsilon)$ which determines the probability of the system changing from state ε to state X assuming that a transition has occurred. The probability of a transition occurring at any instant of time is given by the function $\lambda(\varepsilon)$ which depends only on the state variable ε. The fundamental assumption of the Markov process is that the state variable ε contains all the possible information that we can know about the system at any instant of time and the future evolution of this variable depends only on its present state and not on how it had reached this state.

In applying this model to aftershock occurrences, it is assumed that the state variable is the amount of accumulated strain energy to be released. An aftershock represents a transition from state ε to a lower state X. The magnitude of the earthquake is directly related to the difference of energies between these two states.

The model has been intensely studied in the earthquake literature. The mathematical implications of the model were examined by Aki (1956, and Vere-Jones (1966, 1970). The main mathematical difficulty was finding a suitable transition function $T(X|\varepsilon)$ that duplicated the frequency magnitude relation of earthquakes and aftershocks. Knopoff (1971) and Knopoff et al. (1972) applied this model to a laboratory model of earthquake occurrences. Filson (1973) has tested this model on the earthquake sequence associated with the eruptions in the Galapagos Islands.

In this paper we find suitable transition functions and $T(X|\varepsilon)$ that duplicate the known empirical relations on aftershock occurrences. The model is tested by Monte Carlo simulation using a random number generator. In the second part of the paper the model is extended to describe both the occurrences of independent earthquakes and their associated aftershocks by embedding the Markov process into a stationary branching Poisson process.

MARKOV MODEL

The statistical characteristics of this model are determined by two functions $\lambda(\varepsilon)dt$, the probability of a transition occurring from state ε in an infinitesimal time interval between t and t + dt, and $T(X|\varepsilon)dX$, the probability of jumping from energy state ε to an energy level between X and X+dX given that a jump occurred. Kolmogorov (1931) showed that the probability of being in state ε at time t, $P(\varepsilon,t)$ is a solution of the integrodifferential equation

$$\lambda(\varepsilon)P(\varepsilon,t)+\frac{\partial P(\varepsilon,t)}{\partial t} = \int P(X,t)\lambda(X)T(X|\varepsilon)dX \qquad (1)$$

In order to test the suitability of this Markov model it was necessary to determine the nature of these functions $\lambda(\varepsilon)$ and

$T(X|\varepsilon)$. The mathematical difficulties involved in solving equation (1) limit one to simple functions using a trial and error procedure, and to applying computer simulations using Monte Carlo methods.

To find suitable functions for $\lambda(\varepsilon)$ and $T(X|\varepsilon)$ we utilize some observed properties of earthquakes. The function $T(X|\varepsilon)$ controls the energy (magnitude) distribution of earthquakes while the function $\lambda(\varepsilon)$ controls the rate that the earthquakes occur in time. The magnitude distribution follows Gutenberg and Richter's frequency magnitude relation (Richter 1958)

$$\log_{10} N(M) = a - bM \tag{2}$$

where $N(M)$ is the number of earthquakes with magnitudes exceeding M, and a and b are empirical constants. Magnitude M can be converted to energy E using (Richter 1958)

$$\log_{10} E = 11.8 + 1.5M \tag{3}$$

From (2) and (3), it follows that the number of shocks having energy E or greater is

$$F(E) = AE^{-B} \tag{4}$$

where $B = b/1.5$, and $\log_{10} A = a + 11.8b/1.5$.

The rate of earthquake occurrences is constant except during an aftershock sequence or earthquake swarm. During an aftershock sequence the rate of earthquakes decays with time t according to Omori's law

$$n(t) = \frac{r}{t^p}\Delta t \tag{5}$$

where n(t) is the expected number of aftershocks in the time interval Δt, and r and p are empirical constants which must be adjusted to a given area and to the time unit (Utsu 1969). An illustration of the degree to which an aftershock sequence obeys this law is illustrated by the Nobi earthquake of 1891 where the aftershock sequence appears to have lasted for nearly 80 years (see Utsu 1969, Fig. 5). Following Vere-Jones (1966), we use these two relationships [equations (4) and (5)] to determine the functions $\lambda(\varepsilon)$ and $T(X|\varepsilon)$.

Both the energy and time distribution of earthquakes [equations (4) and (5)] obey the power laws (Pareto distributions). These laws introduce certain mathematical difficulties. For example, according to equation (4) the number of earthquakes becomes unbounded as E approaches zero. In order to be able to normalize the function to a probabilistic distribution it was necessary to ignore all earthquakes below a certain magnitude. In this case we chose magnitude 4.0 for a cut-off limit since below this magnitude many earthquakes are not detected or reported. Thus it shall be assumed that the probability density function of the energy released in an earthquake is a truncated Pareto distribution

$$\begin{aligned} p(E) &= CE^{-B-1} \qquad E \geq E_o \\ &= 0 \qquad\qquad E < E_o \end{aligned} \tag{6}$$

where C, the normalization coefficient, is determined from

$$\therefore \int_{E_o}^{\infty} p(E) = \frac{-CE^{-B}}{B}\Big|_{E_o}^{\infty} = 1$$

and

$$C = B\,E_o^{\;B} \tag{7}$$

The mean energy of the distribution can be easily determined to be

$$\bar{E} = \frac{BE_o}{B-1} \tag{8}$$

provided $B > 1$. When B is ≤ 1, $\bar{E}$ becomes infinite. This is unphysical since if it were true it would imply that the average energy released by earthquakes is infinite. In order to ensure that $\bar{E}$ is bounded it was necessary that either b in Gutenberg and Richter's frequency magnitude relation is greater than 1.5 or that the magnitude of earthquakes never exceeds a specified value. On account of the fact that b values below 1.5 are very common and that no earthquake of magnitude 9 or greater has been reported, the latter assumption was preferred and used in this treatment.

Taking M_{max} and E_{max} to be the maximum magnitude and corresponding energy of the largest possible earthquake then

$$C = \frac{B}{E_o^{-B} - E_{max}^{-B}}$$

and

$$\overline{E} = \frac{B}{B-1} \cdot \frac{E_{max}^{-B+1} - E_o^{-B+1}}{E_{max}^{-B} - E_o^{-B}} \tag{9}$$

Assuming the model that the energy released in an earthquake is equal to the difference between the energy states X and ε, the frequency distribution of E = ε-X is completely determined by the transition probabilities T(X|ε). On the contrary T(X|ε) is not uniquely determined from the frequency distribution of E. More information is needed on how the energy released by an eartnquake depends on the energy state ε. If the frequency magnitude distribution is invariant with the state of energy of the crust, then there must be no such dependency. Detection of secular changes of b in the frequency magnitude relation have been very difficult to verify on account of the large amount of data required in a small area. Lomnitz (1966) and Hamilton (1966) have indicated that there is no information to the contrary of the hypothesis of "magnitude stability" and that the mean magnitude of earthquakes is independent of time. Such "magnitude stability" must also imply that b is independent of time.

To test the "magnitude stability" we examined the aftershock sequence of the Kern County earthquake of 21 July 1952. The magnitudes of aftershock versus the sequence number of the event as listed in the catalog of earthquakes of Southern California are shown in Fig. 1. The lower graph of the same figure shows the time versus sequence number plot. The first 200 reported events were on the average larger by one magnitude unit than the remaining events in the sequence. However, since the first 200 events were occurring within minutes of each other it is possible that the lower magnitude events were either masked out by the larger events or simply ignored. After the first few days of the aftershock sequence no magnitude instability was apparent despite the dramatic decrease in the aftershock rate.

With the "magnitude stability" and the other assumptions stated earlier we chose the probability transition function to be

$$T(X|\varepsilon) = C(\varepsilon - X)^{-B-1} \qquad E_{max} > \varepsilon - X > E_o$$
$$= 0 \qquad \varepsilon - X < E_o \qquad (10)$$
$$= 0 \qquad \varepsilon - X > E_{max}$$

where C is the normalization constant given by equation (9).

The $\lambda(\varepsilon)$ function was determined on the basis of Omori's law [equation (5)]. It was assumed that at the end of an aftershock sequence the variable ε is zero. To determine $\lambda(\varepsilon)$ the energy was determined as a function of time t by integrating Omori's law and then substituting this relation back into Omori's law. Thus

$$\dot{\varepsilon} = r\bar{E}\int_t^\infty T^{-p} dT$$

$$= \frac{r\bar{E}t^{-p+1}}{p-1} \qquad (11)$$

Solving for t

$$t = \left[\frac{\varepsilon(p-1)}{r\bar{E}}\right]^{1/(p-1)} \qquad (12)$$

and substituting t back into equation (5) gives

$$\lambda(t) = \frac{dn}{dt} = D\varepsilon^q \qquad (13)$$

where

$$q = \frac{p}{p-1}$$

and

$$D = r^{-1/(p-1)}\left(\frac{p-1}{\bar{E}}\right)^{p/(p-1)}.$$

With the functions $\lambda(\varepsilon)$ and $T(X|\varepsilon)$ now known, we were able to test this model by computer simulation using Monte Carlo methods. (Further details on the simulation method are given in the next section.) The distribution of a sample aftershock sequence is shown in Fig. 2a. In this simulation the total energy of all the aftershocks is equivalent to that of one magnitude 8.7 earthquake. The frequency magnitude slope b = 1.0 and Omori's law parameter p = 1.25 were specified. The occurrence time and magnitude of each event were determined by random numbers. The rate parameter $F(\varepsilon)$ was computed to the event on the basis of available energy (ε).

The Markov model as it presently stands explains the known statistical properties of the aftershock occurrences. However, the model does not indicate how the strain energy ε accumulates or how an aftershock sequence ever starts. During the occurrence of an aftershock sequence, the rate of occurrence of aftershocks, λ, varies over several orders of magnitude according to Omori's law. Since λ depends upon the amount of strain energy to be released, ε, and furthermore since the dependence goes as a high power of ε (equation 13), this implies that the strain energy must also vary considerably. An aftershock sequence starts very catastrophically. Just before the main shock, seismic activity may be unnoticeable. The model must be extended in order to simulate the occurrence of the main shock. This is discussed in the next section.

POISSON-MARKOV MODEL

In order to build a model that would explain both the independent earthquakes and their associated aftershocks (if any), the Markov process was embedded into a branching Poisson process (Cox & Miller, 1965; Lewis, 1964).

It was assumed that independent events occur randomly according to a Poisson process with rate Λ. The magnitudes of the independent events were distributed according to Gutenberg and Richter's frequency magnitude relation but not necessarily with the same b value as in the Markov model. A constant fraction f of the energy of each independent event was diverted into the aftershock reservoir ε of the Markov model. If a large magnitude independent event occurred, then sufficient energy was available to generate aftershocks. This energy was released gradually according to Omori's law and Gutenberg-Richter's relation as formulated into the Markov model.

The simulation model was implemented on the computer as follows. Random numbers, U_1, U_2, U_3... uniformly distributed between 0 and 1 were obtained from a random number generator. The time interval t to the next Poisson event was determined from

$$t = -\ln(U_1)/\Lambda \tag{14}$$

where ln is natural loganthm.
This transformation ensures that the time intervals between the events are exponentially distributed. The magnitude of this event was determined from

$$M = M_{min} - \frac{\ln(U_2)}{b_i} \tag{15}$$

where M_{min} is the minimum magnitude considered, ensuring a linear log N (frequency) versus M (magnitude) relation. The energy equivalent to this magnitude was determined from equation (3). A fixed fraction f of this energy was added to the aftershock energy reservoir ε .

The aftershock process was simulated as follows. The rate function λ was determined from equation (12). The time interval to the next aftershock was determined from

$$t = -\ln(U_i)/\lambda \qquad (16)$$

and the magnitude from

$$M = M_{min} - \frac{\ln(U_{i+1})}{b_a} \qquad (17)$$

The magnitude of the aftershock was converted back to energy and subtracted from ε. Provided ε was not less than zero, λ was recalculated and the next aftershock was generated.

In our Monte-Carlo simulation of this process we chose the following parameters: Poisson rate $\Lambda = 0.1$; Omori parameters [equation (5)] $p = 4/3$, $r = 2$; fraction of energy going into aftershocks $f = 0.4$; b values for the frequency-magnitude relationship [equation (2)] for aftershocks $b_a = 1.1$, for independent events $b_i = 0.9$; and maximum and minimum magnitudes $M_{max} = 8.0$ and $M_{min} = 4.0$. Sample plots of two such simulations are given in Figs. 3 and 4.

Two examples of catalogs of events generated by this process are shown in Fig. 3. The magnitudes of events (both independent earthquakes and aftershocks or Markov dependent events) are shown as a function of time. The aftershock sequences after large independent earthquakes are quite clear. The sequences very much resemble the actual earthquake catalogs. They have nearly all the statistical characteristics of earthquake catalogs. Omori's law was valid for the large aftershock sequence, and the frequency-magnitude relation was similar to actual events as shown in Fig. 4. Cumulative log N versus M plots are very much like those obtained from earthquake data. The constant value below magnitude 4 is because, in the simulation, $M = 4$ was taken as the minimum magnitude and no earthquakes were considered below this value.

Earthquake swarms were not generated in this model. The model could be modified to generate an earthquake swarm by addition of energy for a fixed period of time into ε at a constant rate. The added energy would increase the rate λ of events generated for that time yielding the appearance of an earthquake swarm.

CONCLUSIONS

A stochastic model was developed to describe both the magnitude and time occurrences of aftershocks and earthquakes. The aftershock occurrences were simulated by a continuous state, continuous time, jump Markov process where the state variable was the unreleased strain energy. The transition and rate functions were determined by constraining the model to preserve Omori's relation on the decay of an aftershock sequence and Gutenberg and Richter's frequency magnitude relation. It was found that the rate function must go as a high power of the strain energy and the transition function $T(X|\varepsilon)$ must be defined by a truncated Pareto distribution for $E = \varepsilon - X$.

In order to explain both the aftershock sequences and the main (independent) earthquakes, the Markov process was embedded into a branching Poisson process. Independent events were assumed to occur as a stationary Poisson process with a truncated Pareto energy distribution. A fixed portion of the energy of the independent event was assumed to be unreleased and transferred to the energy reservoir ε of the aftershocks. As a result a large main event could trigger a series of aftershocks which would release this energy according to a Markov process.

The model is generally successful in describing the known statistical properties of earthquakes and aftershocks. The model differs from actual event occurrences in one particular respect, namely, that a large magnitude aftershock could completely exhaust the energy reservoir and stop all future occurrence of aftershocks associated with the given main event. This may not necessarily be the fault of the branching model but rather the artificial distinction between independent events which can generate aftershocks and the aftershocks which cannot.

ACKNOWLEDGMENTS

We would like to thank Dr. John Filson of Lincoln Laboratory for the discussions that stimulated this work. Also we would like to thank Prof. C. Allin Cornell for providing us with a magnetic tape of the earthquake catalog in Southern California. Computations were carried out at Lincoln Laboratory's Seismic Discrimination Group computers.

This work was supported by the National Oceanic and Atmospheric Administration under Contract N22-163-72-G.

REFERENCES

Aki, K. (1956). Some problems in statistical seismology, Zisin 8, 205-228.

Algermissen, S.T. (1969). Seismic risk studies in the U.S., 4th World Conference of Earthquake Engineering, Vol. 1, 14-27.

Cornell, C.A. (1968). Engineering seismic risk analysis, Bull. Seism. Soc. Am. 58, 1583-1606.

Cox, D.R. and H.D. Miller (1965). The Theory of Stochastic Processes. Methuen.

Filson, J. (1973). A stochastic model and a real earthquake swarm (abstract only). Trans. Am. Geophys. Un. 54, no. 4.

Hamilton, C.A. (1966). The Fiordland earthquake sequence of 1960 and seismic velocities beneath New Zealand, N. Z. J. Geol. Geophys. 9, 224-238.

Knopoff, L. (1971). A stochastic model for the occurrence of main-sequence earthquakes. Rev. Geophys. 9, 175-188.

Knopoff, L., R. Mitchel and D.D. Jackson (1972). A stochastic analysis of a model earthquake sequence, Geophys. J. R. Astron. Soc. 29, 225-261.

Kolmogorov (1931. a Über die analytischen methoden in der wahrscheinlichkeitsrechnung. Math. Ann. 104, 415-458.

Lewis, P.A.W. (1964). A branching Poisson model for the analysis of computer failure patterns. J. Roy. Stat. Soc. B. 26, 398-456.

Lomnitz, C.A. (1966). Magnitude stability in earthquake sequences, Bull. Seism. Soc. Am. 56, 247-249.

Milne, W.G. and A.G. Davenport (1969). Distribution of earthquake risk in Canada, Bull. Seism. Soc. Am. 59, 729-754.

Mogi, K. (1967). Earthquakes and fractures, Tectonophysics 5, 35-55.

Richter, C.G. (1958). Elementary Seismology, Freeman.

Shlien, S., and M.N. Toksöz (1970). A clustering model for earthquake occurrences, Bull. Seism. Soc. Am. 60, 1765-1787, 1970.

Utsu, T. (1969). Aftershocks and earthquake statistics I, J. Faculty of Science, Hokkaido University of Geophysics, Series 3, 129-195.

Vere-Jones, D. (1966). A Markov model for aftershock occurrences, Pure and Applied Geophysics, 64, 31-42.

Vere-Jones, D. (1970). Stochastic models for earthquake occurrences. J. Roy. Stat. Soc. B 32, 1-62.

Figure Captions

Fig. 1 Top: magnitude versus sequence number of events in the Kern County area starting from January 1952. The arrow indicates the main shock. Bottom: time in months versus sequence number of events in the Kern County area.

Fig. 2a Top: magnitude versus time (in arbitrary units) of a simulated aftershock sequence. Bottom: percent of aftershocks which are yet to occur plotted as function of time (arbitrary units).

Fig. 2b Cumulative frequency magnitude distribution of the simulated aftershock sequence shown in Fig. 2a.

Fig. 3 Two examples of computer simulation of earthquakes using the compound Poisson-Markov models. Magnitudes versus time of independent Poisson events (earthquakes) and their Markov dependent events (aftershocks) are shown.

Fig. 4 Cumulative frequency magnitude distribution of events generated by computer simulations and shown in Fig. 3.

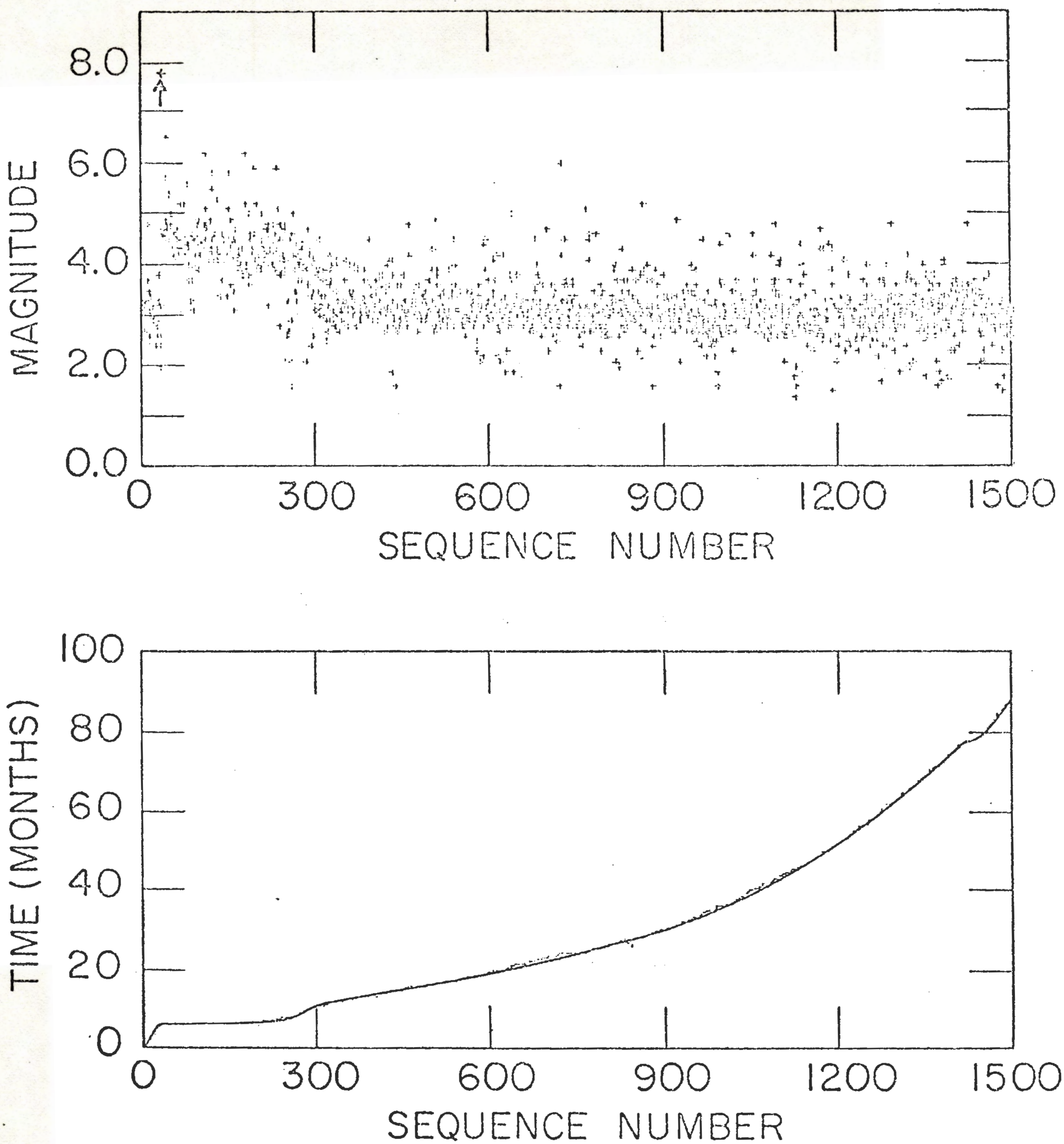
MAGNITUDE
8.0
6.0
4.0
2.0
0.0
0
300
600
900
1200
1500
SEQUENCE NUMBER
TIME (MONTHS)
100
80
60
40
20
0
0
300
600
900
1200
1500
SEQUENCE NUMBER

Fig. 1

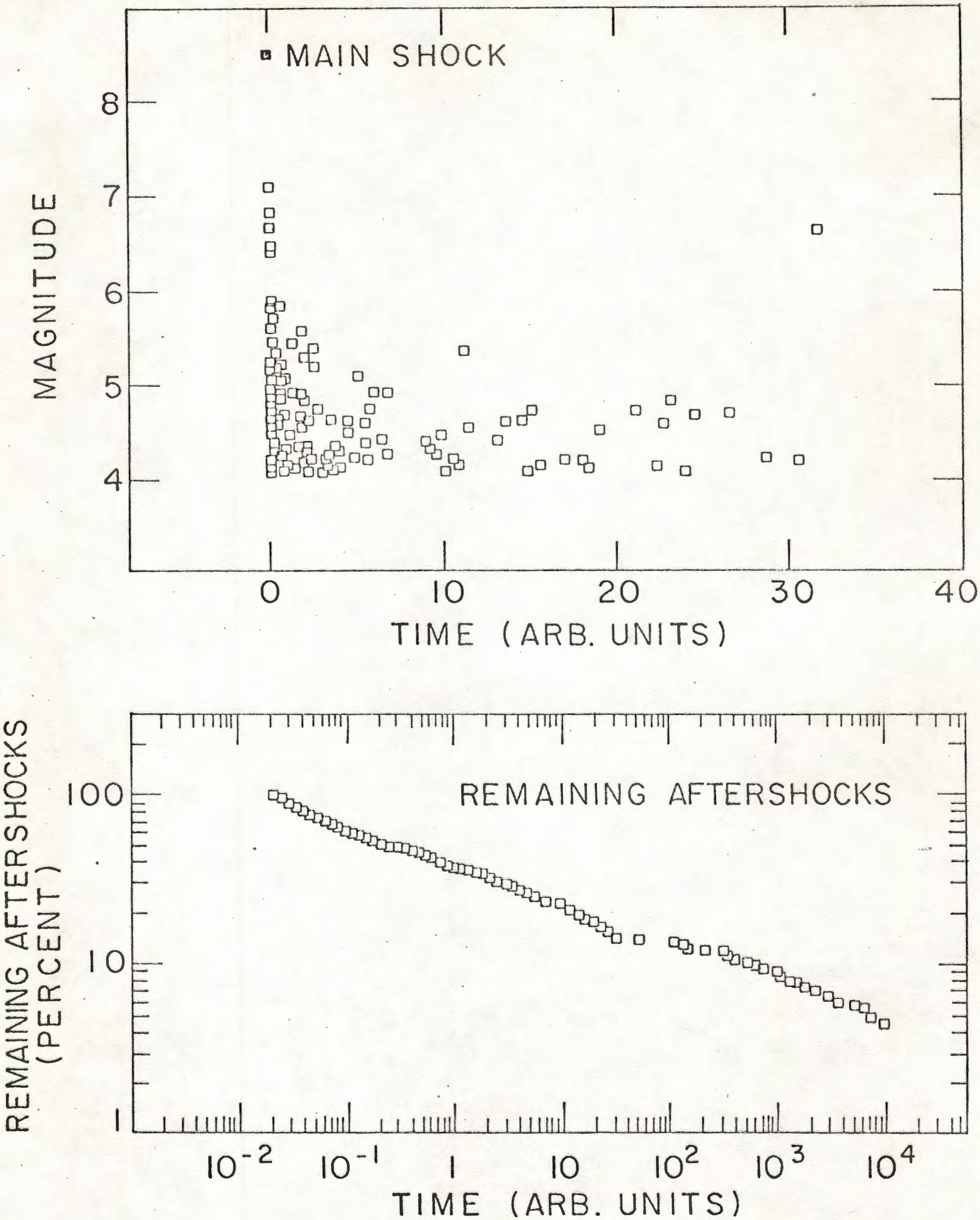
MAIN SHOCK
MAGNITUDE
8
7
6
5
4
0
10
20
30
40
TIME (ARB. UNITS)
REMAINING AFTERSHOCKS
REMAINING AFTERSHOCKS (PERCENT)
100
10
1
10^{-2}
10^{-1}
1
10
10^{2}
10^{3}
10^{4}
TIME (ARB. UNITS)

Fig. 2a

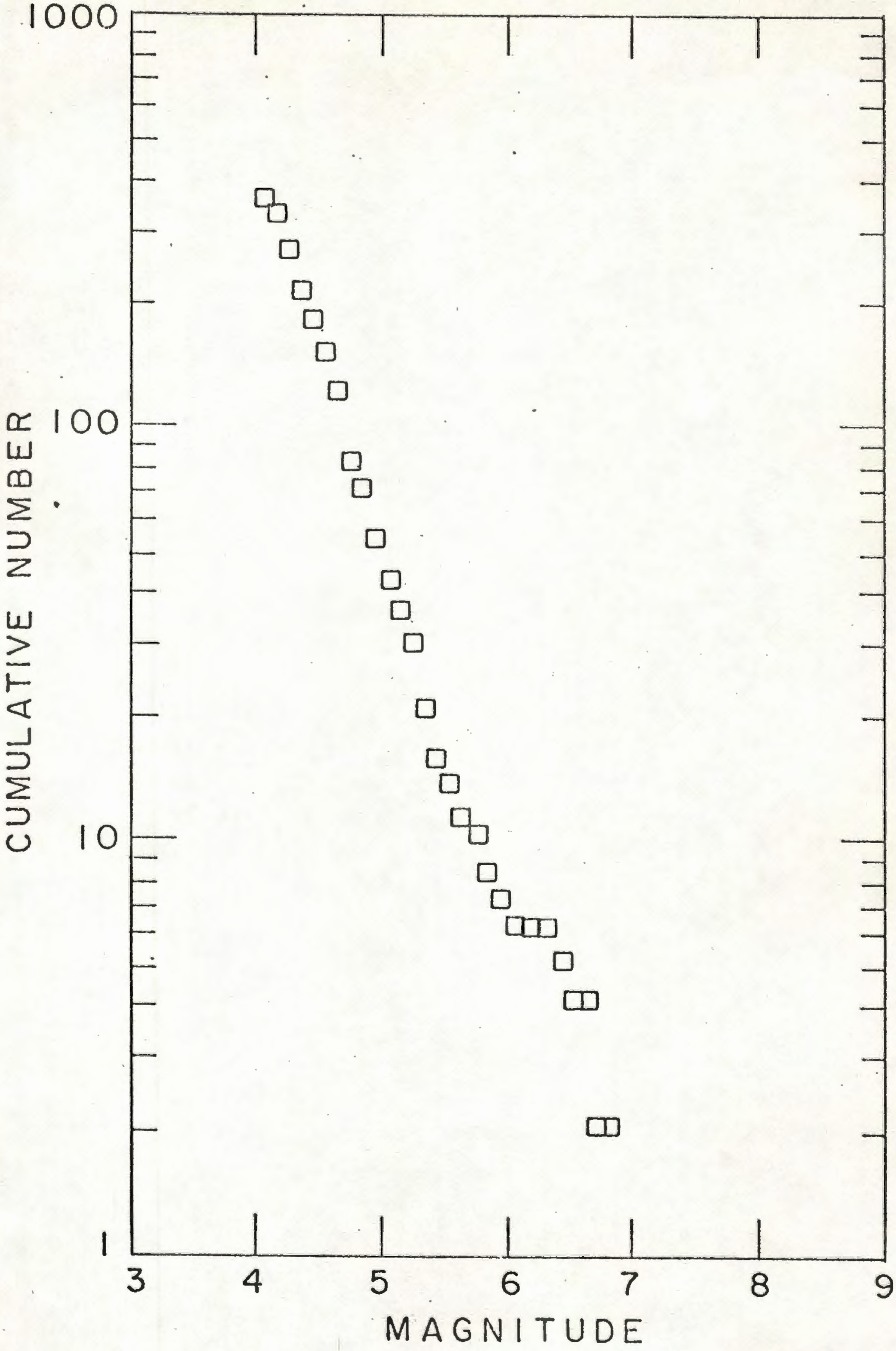

Fig. 2b

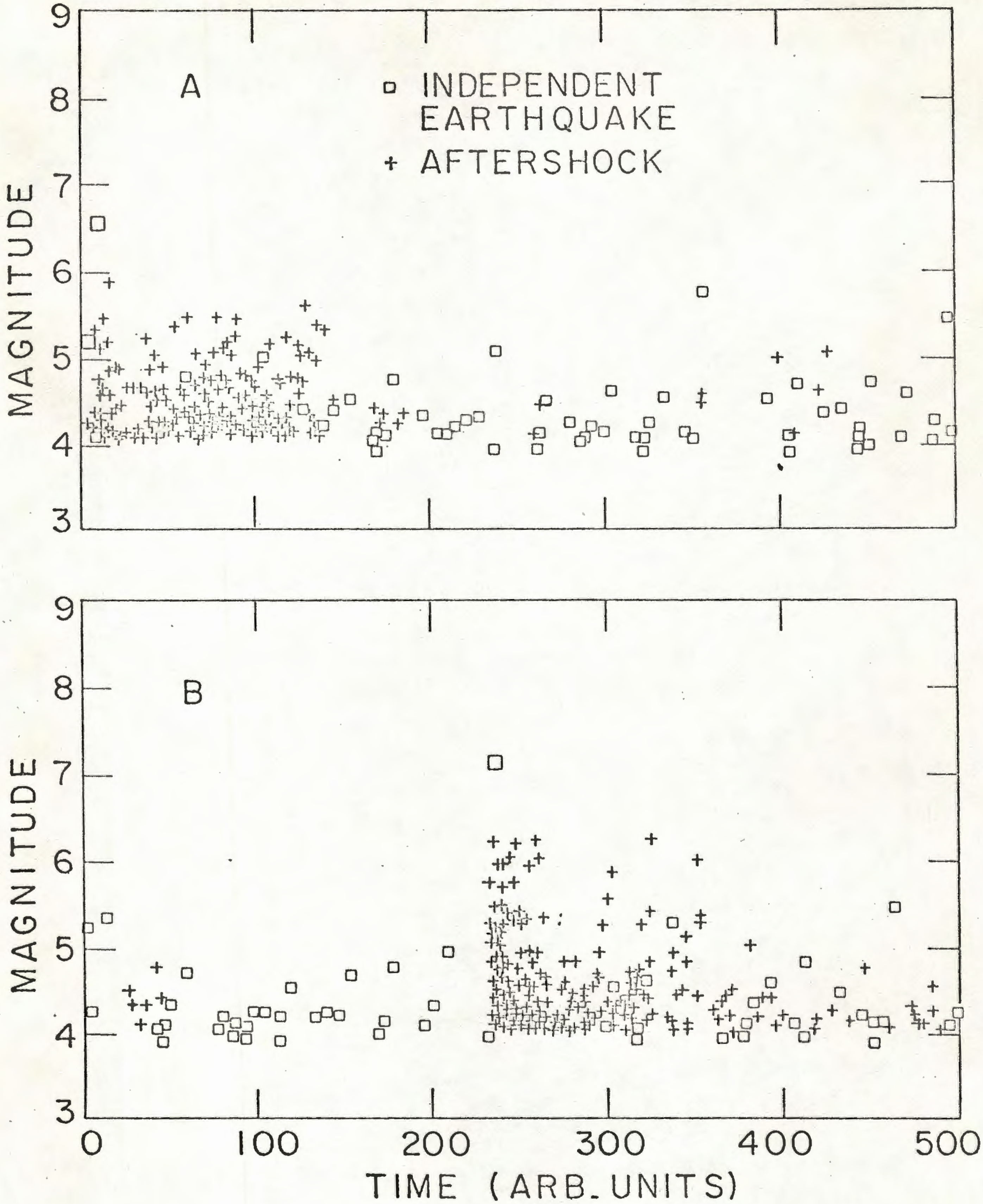
A
INDEPENDENT EARTHQUAKE
AFTERSHOCK
MAGNITUDE
B
TIME (ARB. UNITS)
0
100
200
300
400
500
3
4
5
6
7
8
9

Fig. 3

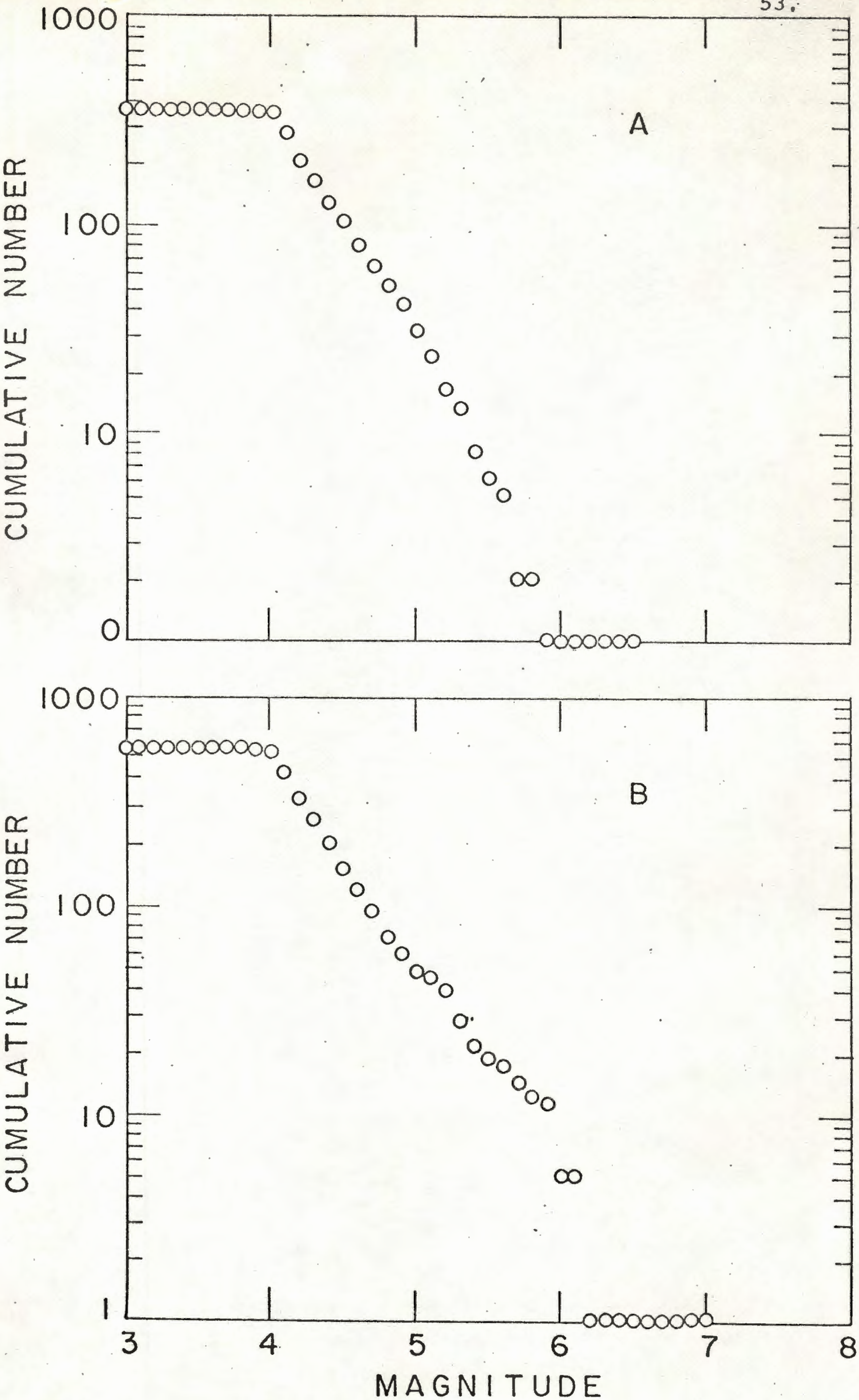

Fig. 4

IV. PAPERS SUBMITTED FOR PUBLICATION

Shlien, S. and M.N. Toksöz, A statistical method of identifying dependent events and earthquake aftershocks, Earthquake Notes, 45, 3-16, 1974.

Shlien, S. and M.N. Toksöz, A branching Poisson-Markov model of earthquake occurrences, Geophys. J., in press, 1974.